A NOVEL COMMAND CONCEPT FOR SIMPLIFIED VEHICLE OPERATIONS OF ONBOARD PILOTED VTOL TRANSITION AIRCRAFT

J. Angelov*, F.Holzapfel†

* Technical Usiversity of Munich, Institute of Flight System Dynamics, Boltzmannstr. 15, Garching near Munich, Germany

† Technical Usiversity of Munich, Institute of Flight System Dynamics, Boltzmannstr. 15, Garching near Munich, Germany

Abstract

In this paper a novel command concept for onboard piloted vertical take-off and landing (VTOL) transition aircraft is introduced. The focus lies in providing an easy and intuitive operational concept for transition aircraft, thereby minimizing the required training before and workload during operation of such a novel configuration. The proposed operational concept is realized using a novel type of control inceptor, which combines the characteristics of spring-centered sidesticks and throttle levers. Model-based simulation and analysis serve as a means of concept validation.

1. INTRODUCTION

Disruptive innovations in the area of electric propulsion, batteries, power electronics, and embedded computer systems are opening up a new era of air mobility [1] [2]. Specifically, rapid advances in the development of electric *vertical take-off and landing* (VTOL) aircraft are a key enabler for new types of missions and application scenarios, which are not feasible or not economical using existing vehicle concepts. Improving accessibility of remote areas, alleviating urban traffic congestion, or enabling faster and more economical transportation means for first responders represent some of the driving forces that have brought worldwide attention to electric VTOL aircraft (Figure 1) [3] [4] [5] [6] [7] [8].

FIG 1. Electric VTOL aircraft. Top row: **Joby S4, Kitty Hawk Cora, Lilium Jet.** Bottom row: **Voloconnect, Volocity, Aurora PAV** (Sources: Company sites and evtol.news)

Extensive use of embedded computer systems and sensor technology enables a high degree of flight control automation and augmentation, which improves the handling of such new type of aircraft or makes it even possible in the first place. The concept of *Simplified Vehicle Operations* (SVO) leads to lower qualification requirements for the pilot and significantly reduces both the training time before as well as the workload during operation of the VTOL aircraft [9] [10] [11].

In the following a behavioral specification for onboard piloted VTOL transition aircraft is proposed. The resulting Simplified Vehicle Operations are motivated by the concepts presented in [12] and [10]. Modifications and adaptations are introduced to account for a novel control inceptor design (see [11]) and improve the handling, judged by virtual flight tests conducted in [13].

The goal is a behavioral concept that is compatible with lift and cruise configurations (but with some modifications also for tilting propulsion concepts) and that reduces the requirements on the skill level of the aircraft operator to a minimum through highly automated closed-loop control of the transition vehicle throughout the whole flight envelope. The operational concept is aimed at yielding intuitive response behavior of the transition aircraft to control inputs, thereby enabling safe and efficient completion of applicable missions, some of which can be found in [14] (in the form of Mission Task Elements).

The proposed Simplified Vehicle Operations are motivated by existing concepts like 'Unified' [15] (developed by UK's Royal Aircraft Establishment in the 1970's and 80's) and 'E-Z-Fly' [16] (developed at NASA Langley in the 1990's), which are also mentioned and described in [10], however modifications and adaptations are introduced to account for the novel control inceptor design in figure 2 while preserving good handling qualities.

The proposed behavioral concept of the VTOL transition aircraft shall be realized by highly automated closed-loop control throughout the whole flight enve-

doi: 10.25967/550011

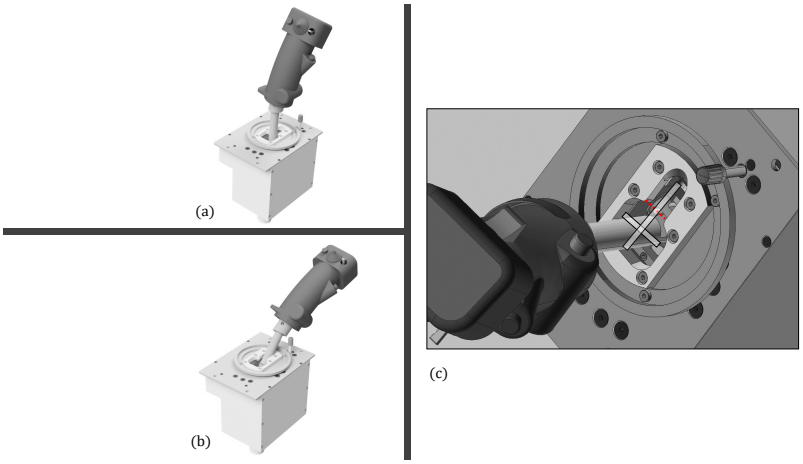

FIG 2. Left Control Inceptor in Spring-Centered Position (a), in Throttle Lever Position (b), and Close-Up of the Detent Notch (c)

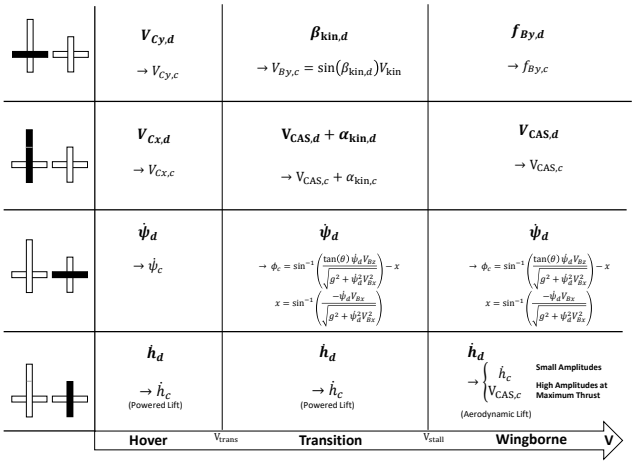

FIG 3. SVO Table: Command and Target Variables During Hover, Transition, and Wingborne Flight

lope: from low speed hovering through the medium speed transition phase into the high speed wingborne phase. The main objective is enabling safe and efficient completion of typical missions like the Mission Task Elements (MTE) described in [14] and novel mission scenarios resulting from the transition capability of the aircraft. The proposed operational concept avoids mode confusion of the operator and provides consistent aircraft response to control inceptor deflections at every flight speed.

Operation is realized with two control inceptors: a passive side stick on the right and a passive sidestick on the left, which extends forward into a non-spring-centered region, mimicking a thrust lever. Figure 2 shows the novel control inceptor design, which was first mentioned in [11] and has been used in virtual flight test studies in [11] and [13].

The mapping from inceptor deflection to command as well as the choice of internally tracked target variables are chosen such as to provide good handling qualities in every flight condition and to account for flight envelope protections such that the commands do not exceed the physical capabilities of the vehicle in any given flight situation. An overview of the command concept can be found in figure 3.

The behavioral specification of the transition vehicle is divided into three phases, which are distinguished by vehicle velocity (and dynamic pressure) and motivated by different kinematic and kinetic characteristics of low, medium, and high velocity operation of the VTOL aircraft. The internally tracked variables as well as allocation of forces and moments are adapted to the current flight phase, however, the response of the transition aircraft to control inceptor inputs remains consistent throughout the entire flight envelope as can be seen in figure 3.

2. SIMPLIFIED VEHICLE OPERATIONS OF VTOL TRANSITION AIRCRAFT

2.1. Low Velocity Operation: Hover

The control concept for low velocity operation of the transition aircraft is driven by the requirements of relative translational control with respect to earth-fixed objects. The Aeronautical Design Standard ADS-33E-PRF [14] defines performance specifications and handling quality requirements for military rotocraft as well as typical operational missions in form of Mission-Task-Elements (MTEs) that represent the entire spectrum of intended operational usage and serve as behavioral basis for the control concept that is described in the following. Note that the applicability of conventional rotorcraft requirements on VTOL transition configurations has to be considered on an individual basis and will ultimately be validated in terms of model-based simulation.

2.1.1. Left Longitudinal and Lateral Stick Channel During Hover Phase

Using the left control inceptor the operator commands a horizontal translational rate with respect to ground. The target translational rate is defined as velocity vector in the control frame, which is shown in figure 4. The control frame is horizontal to the earth surface and aligned with the heading of the VTOL aircraft, i.e. the north-east-down frame rotated by the heading angle of the vehicle. In order to achieve good handling qualities, ADS-33E-PRF specifies the boundaries for the relationship between applied cockpit control force and the resulting target translational rate, which is shown in figure 6.

Motivated by one of the central control guidelines mentioned in [15], the movement of the transition vehicle should generally follow the control inceptor deflection. Hence, the deflection of the left control inceptor determines the direction of the target translational rate by mapping the stick direction in

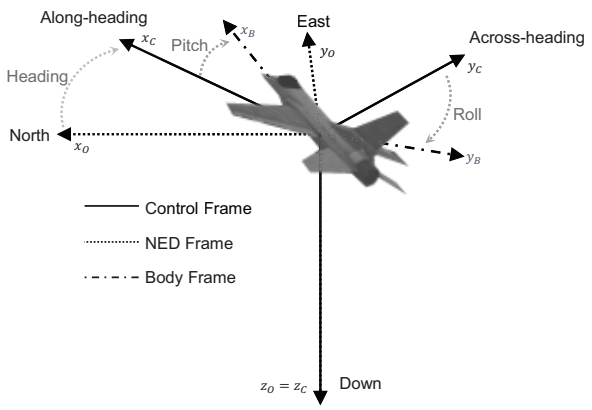

FIG 4. Coordinate Frames

inceptor-fixed coordinates (subscript S) into the control frame (subscript C) as can be seen in figure 5. Longitudinal and lateral stick deflections therefore correspond to along-heading and across-heading movement of the aircraft.
In order to achieve direction-preserving properties for the mapping of stick deflection $(\boldsymbol{d})_S = \begin{bmatrix} d_{Sx} & d_{Sy} \end{bmatrix}_S^T$ to target velocity $(\boldsymbol{V}_{\text{hor},c})_C = \begin{bmatrix} V_{Cx,c} & V_{Cy,c} \end{bmatrix}_C^T$, the following relationship has to be satisfied:

(1) $$\tan(\beta_C) = \frac{V_{Cy,c}(d_{Sy})}{V_{Cx,c}(d_{Sx})} = \frac{d_{Sy}}{d_{Sx}} = \tan(\beta_S) \,,$$

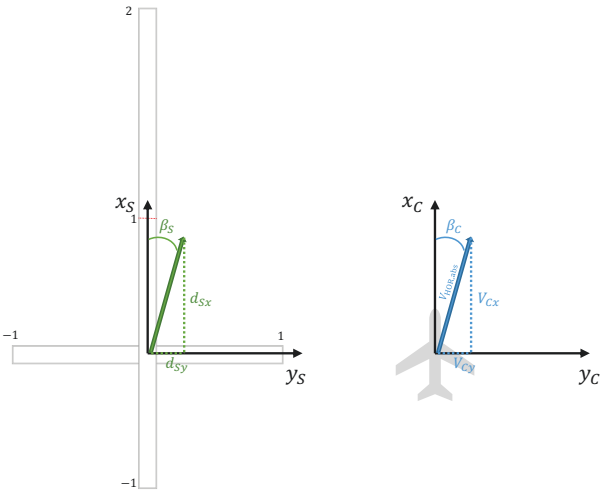

FIG 5. Mapping of Left Control Inceptor to Translational Rate During Hover Flight

Note that dependent on the force characteristics of the stick, it might be necessary to introduce a nonlinear mapping from stick deflection to translational rate, such that the stick force to translational rate requirements from figure 6 are met. Furthermore, in order to satisfy the direction constraint (1), the target velocity is expressed in terms of polar coordinates

(2) $$V_{Cx} = \cos(\beta_C) V_{\text{HOR,abs}} \quad V_{Cy} = \sin(\beta_C) V_{\text{HOR,abs}} \,,$$

with the translational direction β_C and translational rate $V_{\text{HOR,abs}}$ being expressed in terms of the stick deflection according to

(3) $$\beta_C = \beta_S = \operatorname{atan2}(d_{Sy}, d_{Sx}) \quad V_{\text{HOR,abs}} = f(d_{Sx}, d_{Sy}) \,.$$

The function f in (3) determines the relationship between absolute stick deflection and target translational rate. In case of a constant and omnidirectional stick spring constant $C_{\text{spring}} = \frac{F_{\text{stick,lb}}}{\sqrt{d_{Sx}^2 + d_{Sy}^2}}$, which denotes the stick force in pounds for a unit deflection in stick coordinates $(\boldsymbol{d})_S$, the quadratic function

(4) $$f(d_{Sx}, d_{Sy}) = a C_{\text{spring}}^2 \left(d_{Sx}^2 + d_{Sy}^2\right) + b C_{\text{spring}} \sqrt{d_{Sx}^2 + d_{Sy}^2} \,,$$

(5) $$a \approx 0.83 \, \frac{ft/s}{lb^2} \,,$$

(6) $$b \approx 5.83 \, \frac{ft/s}{lb} \,,$$

is located between the boundaries in figure 6c and therefore yields Level 1 handling qualities. Furthermore, the maximum forward velocity in hover is denoted as V_{hover} and represents the border between hover operation and the transition phase.

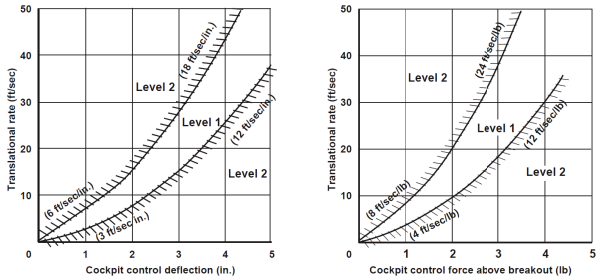

b) Control/response requirement for centerstick controllers

c) Control/response requirement for sidestick controllers

FIG 6. Cockpit Control Deflection/Force Versus Translational Rate According to ADS-33E-PRF [14]

Upon releasing the left control inceptor the system controls the translational rate to zero and holds the horizontal position with respect to ground, thereby compensating position drift, e.g. due to wind gusts.

2.1.2. Right Longitudinal Stick Channel During Hover Phase

Deflections along the longitudinal direction of the right control inceptor are interpreted as a target vertical velocity $\dot{h}_d = -V_{Cz,c}$. Pulling or pushing the stick initiates a climb or descent rate respectively. Upon releasing the right stick, the VTOL aircraft stops the vertical motion and starts to hold the current height (above ground). Flight simulator tests conducted in

[11] suggest that, if the longitudinal breakout force of the right stick during lateral deflections is not significant enough, a dead-zone in the longitudinal channel is necessary in order to account for undesired height changes during lateral deflections.
According to [14], the minimum climb and sink rate characteristics during hover have to satisfy the requirements in table 1. When operating close to the

TAB 1. Vertical Rate Requirements During Hover Flight [14]

Handling Quality Level	Minimum Vertical Rate[1]
Level 1	$160\,ft/min$
Level 2	$55\,ft/min$
Level 3	$40\,ft/min$

[1] achievable vertical rate 1.5 seconds after initiation of a rapid displacement

ground, the sink rate is limited based on the height above ground level h_{AGL} according to

$$\dot{h}_{\mathsf{min}} = -V_{Cz,\mathsf{max}} = \frac{1}{T_h}\left(h_{\mathsf{TH}} - h_{\mathsf{AGL}}\right)\,, \tag{7}$$

in order to avoid unintentional flight into ground. Hence, the height above ground converges on the target height $h_{\mathsf{TH}} < 0$ with a time constant of T_h. A negative target height is chosen, such as to maintain a minimum sink rate capability of $\frac{h_{\mathsf{TH}}}{T_h}$ when touching the ground.

2.1.3. Right Lateral Stick Channel During Hover Phase

The lateral axis of the right control inceptor is interpreted as a desired heading rate $\dot{\psi}_d$. Deflecting the stick to the left or right will result in a negative or positive heading rate respectively. Depending on the agility category, table 2 shows the required performance limits to achieve Level 1 or Level 2 and 3 handling qualities.
Upon releasing the right stick, the VTOL aircraft shall hold the current heading. However, it might be necessary to give up the heading hold functionality in the presence of strong steady state wind due to the limited yaw authority of typical VTOL configurations compared to tail rotor configurations. Additionally, the presence of a tail rudder used for lateral control during wingborne flight increases the sensitivity to lateral gusts during hover flight.

TAB 2. Heading Rate Requirements During Hover Flight [14]

Agility Category	Achievable Heading Rate	
	Level 1	Level 2 and 3
Limited Agility	$\pm 9.5\,deg/s$	$\pm 5\,deg/s$
Moderate Agility	$\pm 22\,deg/s$	$\pm 9.5\,deg/s$
Aggressive Agility	$\pm 60\,deg/s$	$\pm 22\,deg/s$

Since the left control inceptor defines the target velocity vector in the heading-fixed control frame, a demand in heading rate requires curvature of the kinematic velocity and acceleration in the horizontal plane has to be provided by the system. Due to the lack of lateral force capability, this maneuver requires a change in vehicle attitude in order to tilt the lift vector into the horizontal plane. As a consequence, an input in the right lateral stick channel during forward flight leads to a kinematically coordinated bank-to-turn maneuver. However, the coordination happens with respect to the across-heading velocity rather than the body lateral velocity.
In this context it also has to be considered, up to which velocity V_{Cx} the target heading rate $\dot{\psi}_d$ can be supported by the system's lift performance and hence its capability of horizontally curving the velocity vector while maintaining sufficient vertical acceleration authority $\ddot{h}_{\mathsf{req}}$. The equations of motion in z_C and y_C direction during a steady turn with velocity $V_{Cx} = \text{const}$ are given respectively by

$$\dot{V}_{Cz} = -\ddot{h} = \cos(\phi)\cos(\theta) f_{Bz} + g \tag{8}$$

and

$$\dot{V}_{Cy} = 0 = -\sin(\phi) f_{Bz} - \dot{\psi} V_{Cx}\,, \tag{9}$$

with f_{Bz} denoting the specific force in body-vertical direction, ϕ and θ denoting the roll and pitch angle respectively, and g denoting the gravitational acceleration. The influence of the traction system on the vertical channel is neglected due to small pitch angles.
Hence, given the maximum specific lift force $f_{\mathsf{max}} = -f_{zB,\mathsf{min}} > 0$ that the system can produce and assuming small pitch angles θ, the maximum absolute target heading rate $\dot{\psi}_{\mathsf{abs,max}}$ at a given velocity V_{Cx} yields

$$\dot{\psi}_{\mathsf{abs,max}} = \frac{1}{V_{Cx}}\sqrt{f_{\mathsf{max}}^2 - \left(\ddot{h}_{\mathsf{req}} + g\right)^2}\,, \tag{10}$$

while considering a required minimum authority in vertical acceleration $\ddot{h}_{\mathsf{req}}$.
Note that the roll response during a change in heading indirectly occurs as a consequence of controlling and stabilizing the across-heading velocity component and is therefore coupled to the heading channel (bank-by-turn characteristic). This represents a different paradigm than for medium and high velocity operation, where the yaw response is governed by the lateral components of the velocity vector (or resulting lateral load factor due to aerodynamic forces) and hence is a consequence of the directly controlled roll angle (bank-to-turn characteristic).

2.2. Medium Velocity Operation: Transition

The transition phase starts after the VTOL aircraft reaches a kinematic velocity of $V_{Cx} = V_{\mathsf{hover}}$ and the left stick is located behind the detent notch in the throttle lever area, denoted by the red dotted line in figure 2. Furthermore, in order to switch back

to the hover phase, the velocity has to $V_{Cx} = V_{\text{hover}} - \Delta V$ and the stick has t before the notch. The threshold ΔV a hysteresis to avoid limit cycles at t both modes. The moding logic is ada In order to avoid mode confusion of the mapping of control inceptor channe variables during the transition phase is as to provide similar behavior of the VT for the hover phase. However, the choic tracked variables is adapted to the cha medium to high velocity operation.

2.2.1. Left Longitudinal Stick Cha Transition Phase

The proposed mapping of the left contr driven by the following requirements during the transition phase:

1) The aircraft response to control inceptor deflections during transition shall be similar to hover and wingborne flight.
2) Transition into the wingborne phase shall happen at a defined angle of attack and airspeed during horizontal and straight flight.
3) There shall be sufficient margin towards stall when switching to the wingborne phase.
4) Acceleration shall be provided by the forward propulsion system rather than pitching down.
5) Deceleration of the aircraft shall be supported by respective pitch up movement at low dynamic pressures.
6) The authority to actively command changes in angle of attack shall be reduced at high dynamic pressures in order to avoid coupling with the powered lift system in the vertical channel and mitigate excessive loads.
7) The maximum airspeed shall be limited during transition in order to avoid excessive loads on the high power lift system.

Similarly to the hover phase, the longitudinal channel of the left stick corresponds to a velocity command during the transition phase. However, instead of the kinematic velocity with respect to earth, the indicated airspeed $V_{\text{CAS},d}$ is controlled through automatic command of forward thrust at a predefined kinematic angle of attack $\alpha_{\text{kin},d}$. Both the airspeed and the angle of attack are determined based on the position of the left control inceptor and the current airspeed as is qualitatively shown in figure 7.

Right behind the detent notch the commanded airspeed is given by $V_{\text{CAS},d} = V_{\text{stall,p}}$, which represents the target speed for the transition into the wingborne phase and is defined as

$$V_{\text{stall,p}} = (1+p)\, V_{\text{stall}}\,, \tag{11}$$

where p is the margin towards stall speed and is chosen around $p \approx 0.2$. Note that the stall speed during the transition phase might be higher than in the wingborne phase due to adverse aerodynamic effects of the (idling) high power lift system.

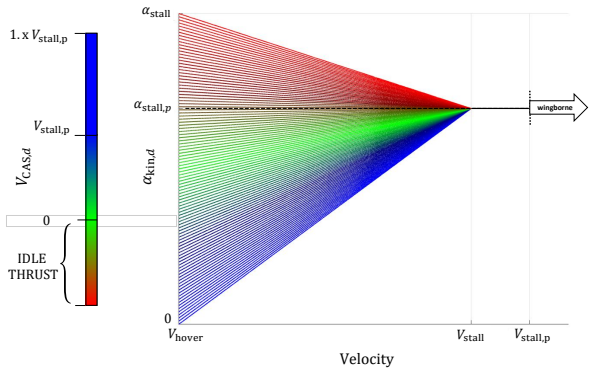

FIG 7. Mapping of Left Control Inceptor During Transition

The corresponding angle of attack

$$\alpha_{\text{stall,p}} = \frac{\alpha_{\text{stall}}}{(1+p)^2} \tag{12}$$

builds up gradually over the speed and yields sufficient lift for horizontal and straight flight at a predetermined air density and velocity of $V_{\text{stall,p}}$ with the high power lift system not providing additional lift.

Below the centered stick position the forward thrust is set to idle and above it the commanded airspeed linearly scales from $V_{\text{CAS},d} = 0$ to $V_{\text{CAS},d} = V_{\text{stall,p}}$ until right behind the detent notch. Since the stick travel while pushing the stick over the detent notch is small but non-zero, the target airspeed below the notch at the upper end of the spring centered stick range corresponds to a value $V_{\text{CAS},d} < V_{\text{stall,p}}$, which represents the maximum speed for which the transition phase can be sustained.

In addition to setting the target airspeed $V_{\text{CAS},d}$, the left stick also sets the target angle of attack $\alpha_{\text{kin},d}$. In line with the requirements stated in the beginning of this section, the target kinematic angle of attack $\alpha_{\text{kin},d}$ linearly scales over the stick range d_{Sx} and velocity V according to

$$\alpha_{\text{kin},d} = \begin{cases} a_\alpha V + b_\alpha, & \text{for } V \le V_{\text{stall}} \\ \alpha_{\text{stall,p}}, & \text{for } V > V_{\text{stall}} \end{cases}, \tag{13}$$

with the parameters a_α and b_α defined according to

$$a_\alpha = \frac{\alpha_{\text{stall,p}} - \alpha_{\text{hover}}}{V_{\text{stall}} - V_{\text{hover}}} \qquad b_\alpha = \alpha_{\text{stall,p}} - a_\alpha V_{\text{stall}} \tag{14}$$

and the kinematic angle of attack at the lower speed boundary of the transition phase given by

$$\alpha_{\text{hover}} = \frac{1 - \min(1, d_{Sx})}{2} \alpha_{\text{stall}}\,. \tag{15}$$

The stick deflection d_{Sx} is defined according to figure 5, where $d_{Sx} = -1$ corresponds to a complete pull of the stick, $d_{Sx} = 1$ corresponds to the upper end of the

spring centered area right before the notch, and $d_{Sx} = 2$ represents a complete push of the stick. Figure 7 shows the two-dimensional relationship is terms of a color-coded mapping.
Upon entering the transition phase and keeping the left control inceptor right behind the notch, the aircraft will level out with respect to the kinematic airflow ($\alpha_{\text{kin},d} = 0$) and start accelerating using the forward propulsion system. While approaching the stall speed V_{stall}, the target angle of attack converges to the margin stalling angle of attack $\alpha_{\text{kin},d} = \alpha_{\text{stall,p}}$ and the high power lift system is close to idle. While flying below the stall speed, pulling the left stick into the spring centered area will - in addition to setting the target airspeed to $V_{\text{CAS},d} = 0$ - increase the angle of attack and support deceleration.
After exceeding the stall speed V_{stall}, the target angle of attack is fixed at the value of $\alpha_{\text{kin},d} = \alpha_{\text{stall,p}}$. Hence, moving the left stick while flying above the stall speed will merely change the target airspeed and hence the commanded thrust but not lead to a change in angle of attack. This strategy supports defined aerodynamic lift conditions before entering the wingborne phase at an airspeed of $V_{\text{stall,p}}$ and avoids generation of excessive loads while the high power lift system is active.
Another measure to avoid excessive aerodynamic loads on the high power lift system is to limit the maximum airspeed during the transition phase. At its maximum forward position the left stick sets the target airspeed to $V_{\text{CAS},d} = 1.x\, V_{\text{stall,p}}$, where x accounts for a desired airspeed margin to get wingborne in the presence of uncertainties. Upon entering the wingborne state full airspeed authority is regained.

2.2.2. Left Lateral Stick Channel During Transition Phase

The left lateral stick channel is mechanically locked above the detent notch. Hence, a constant target value of zero for the lateral body-fixed velocity V_{By} or specific force f_{By} is set during the transition and wingborne phase respectively. However, for the sake of completeness, a possible command mapping is introduced nonetheless, as another control inceptor concept might introduce the possibility to command this channel (e.g. pedals). Note, however, that due to the vertical take-off and landing capability, the need to introduce lateral sideslip conditions is very limited.
The requirement to stabilize the lateral body-fixed velocity during transition is aimed at avoiding cross stream conditions while the high power lift system is active. If a (kinematic) sideslip angle $\beta_{\text{kin}} \neq 0$ during transition is desired nonetheless, the target value for the lateral velocity is set to

$$V_{By,c} = \sin(\beta_{\text{kin},d}) V_{\text{kin}}\,, \tag{16}$$

with V_{kin} being the kinematic absolute velocity.

2.2.3. Right Longitudinal Stick Channel During Transition Phase

The right longitudinal stick channel behaves identically to the hover phase and is interpreted as a desired height rate $\dot{h}_d$. Possible limits in the flight envelope of the vertical channel like translational rates, accelerations, and jerks have to be considered due to higher dynamic pressures.
Note that active control of the kinematic angle of attack based on the left control inceptor position and airspeed leads to an induced pitch response upon commands in the vertical rate channel. Hence, deceleration of the VTOL aircraft can be supported through an additional climb demand, which leads to additional pitch up motion. In order to avoid an excessive pitch response for climb maneuvers at low airspeeds, the angle of attack tracking regime can be replaced with a pitch angle control strategy at lower velocities and blended into controlling the angle of attack for higher airspeeds.

2.2.4. Right Lateral Stick Channel During Transition Phase

Deflections in the right lateral stick channel during transition flight are interpreted as a desired heading rate $\dot{\psi}_d$. However, instead of being directly controlled like in hover mode, the heading rate is the result of a coordinated turn with a target roll angle ϕ_c (i.e. bank to turn). In contrast to the hover phase, the coordination during the transition phase happens with respect to the body lateral velocity component V_{By} due to the requirement of avoiding lateral cross stream while the high power lift system is active.
Although the aircraft's reaction upon lateral deflections of the right control inceptor is very similar to the hover phase, the description of the underlying control mechanism is important in order to fully understand the behavior, also in the presence of disturbances. Compensating lateral velocity deviations by means of yawing rather than a change of lift direction (by rolling) represents a different control paradigm that exploits the fact that with increasing velocity the sensitivity of body-relative accelerations with respect to a change in orientation is increasing. Overall, this behavior is aimed at preserving the velocity direction with respect to earth (or with respect to the air) by rotating the aircraft into the airflow rather than aligning the velocity with the heading of the aircraft.
The derivation of the required target roll angle ϕ_c for a desired heading rate $\dot{\psi}_d$ follows from the constraint of zero lateral body-relative acceleration

$$\dot{V}_{By} = f_{By} + \sin(\phi)\cos(\theta)g - rV_{Bx} + pV_{Bz} = 0\,, \tag{17}$$

where f_{By} denotes the lateral specific force and V_{Bx} and V_{Bz} denote the forward and vertical velocity components in the body frame. The yaw rate r and roll rate p are further expressed in terms of euler angle

rates according to

(18)
$$r = -\sin(\phi)\dot{\theta} + \cos(\phi)\cos(\theta)\dot{\psi} \quad p = \dot{\phi} - \sin(\theta)\dot{\psi}\,.$$

During the stationary turn maneuver the roll and pitch angle remain constant, i.e. $\dot{\phi} = \dot{\theta} = 0$, and the lateral specific force f_{By} is assumed to be zero due to turn coordination and the absence of lateral force capability of the system. In case of wind at higher dynamic pressures, the stabilization smoothly shifts from lateral velocity stabilization to lateral loadfactor stabilization. The lateral body acceleration can furthermore be expressed as

(19)
$$\begin{aligned}\dot{V}_{By} &= 0 \\ &= \sin(\phi)\cos(\theta)g - \cos(\phi)\cos(\theta)\dot{\psi}V_{Bx} - \sin(\theta)\dot{\psi}V_{Bz}\,.\end{aligned}$$

Using the trigonometric identity $a\sin(\phi) + b\cos(\phi) = A\sin(\phi + x)$ with $A = \sqrt{a^2 + b^2}$ and $x = \sin^{-1}\left(\frac{b}{A}\right)$, it follows

(20)
$$A\sin(\phi + x) = \sin(\theta)\dot{\psi}V_{Bz}\,,$$

with $A = \cos(\theta)\sqrt{g^2 + \dot{\psi}^2 V_{Bx}^2}$ and with $x = \sin^{-1}\left(\frac{-\dot{\psi}V_{Bx}}{\sqrt{g^2+\dot{\psi}^2V_{Bx}^2}}\right)$.
Therefore, the required roll angle ϕ_c that leads to a desired heading rate $\dot{\psi}_d$ under the given assumptions yields
(21)
$$\phi_c = \sin^{-1}\left(\frac{\tan(\theta)\dot{\psi}_d V_{Bz}}{\sqrt{g^2 + \dot{\psi}_d^2 V_{Bx}^2}}\right) - \sin^{-1}\left(\frac{-\dot{\psi}_d V_{Bx}}{\sqrt{g^2 + \dot{\psi}_d^2 V_{Bx}^2}}\right).$$

Note that due to the choice of formulating the constraint in terms of the body-fixed lateral direction, the required roll angle follows from a quasi-kinematic relationship and hence only considers the necessary rotation to compensate for the gravity induced lateral acceleration.
The maximum feasible heading rate $\dot{\psi}_d$ under the constraint (19) is derived by considering the minimum required vertical acceleration performance $\ddot{h}_{\text{req}}$ and the available maximum specific lift force $f_{\text{max}} = -f_{zB,\text{min}} > 0$. For small pitch angles it follows from vertical force equilibrium (8) that

(22)
$$\cos(\phi) = \frac{\left(g + \ddot{h}_{\text{req}}\right)}{f_{\text{max}}}\,,$$

which yields the maximum roll angle during a turn, for which the minimum required vertical acceleration $\ddot{h}_{\text{req}}$ is reached at maximum lift force.
Inserting (22) into (19) yields the maximum feasible heading rate

(23)
$$\dot{\psi}_{\text{abs,max}} = \frac{g}{g + \ddot{h}_{\text{req}}}\frac{1}{V_{Bx}}\sqrt{f_{\text{max}}^2 - \left(\ddot{h}_{\text{req}} + g\right)^2}\,.$$

2.3. High Velocity Operation: Wingborne

The transition into the wingborne phase is coupled to various conditions that are discussed in more detail in [17]. In general, the switch into the wingborne phase is initiated when sufficient aerodynamic lift can be provided and the left control inceptor is located behind the detent notch. The powered lift system is subsequently deactivated. Similarly, the re-transition is initiated when the left control inceptor is pulled below the detent notch and the airspeed is sufficiently low.
The command concept for the wingborne mode is targeted at extending the transition phase into high velocity operation. The role of airspeed changes from merely being an independent target variable to becoming a crucial resource for the generation of necessary aerodynamic moments and forces. Therefore, the role of envelope protections becomes particularly important and influences the overall behavioral concept during the wingborne phase.
A thorough description of the control inceptor deflection to aircraft response is given in the following.

2.3.1. Left Longitudinal Stick Channel During Wingborne Phase

Identically to the transition phase, deflections of the left control inceptor during the wingborne phase are interpreted as target indicated airspeed $V_{\text{CAS},d}$. Figure 8 gives an overview of the target airspeed values over the stick range. Just as in the transition phase, the target command at the lower end of the thrust lever region corresponds to the margin stall speed $V_{\text{CAS},d} = V_{\text{stall,p}}$. Below the notch the target airspeed decreases to the stall speed $V_{\text{CAS},d} = V_{\text{stall}}$.
As already mentioned in subsection 2.2, switching to the wingborne mode comes along with a change in maximum command authority for the airspeed, which is limited during the transition phase due to structural integrity of the aircraft and the activated high power lift system. Maximum airspeed authority is completely available upon the mode switch and a full stick deflection corresponds to the maximum airspeed command $V_{\text{CAS},d} = V_{\text{NO}}$ in the wingborne mode. During substantial climb maneuvers, airspeed is traded in for rate of climb, which is discussed in detail within the subsection for the right longitudinal stick channel.
If not properly accounted for, the airspeed command might be subject to a discontinuous change in the moment of engaging the wingborne mode dependent on the stick position. Similar problems arise due to the change in the lower airspeed limit upon switching from wingborne mode back to the transition mode or for any other discrete change in command variables and their limits, as was mentioned for the lateral stick channel of the right stick in the transition phase.
A continuity-based stick mapping is applied to the mode switch between the transition mode and the wingborne mode. The novel input-output mapping ensures that the command output (e.g. the airspeed command) is not subject to a discontinuous jump upon changing the command output limits during

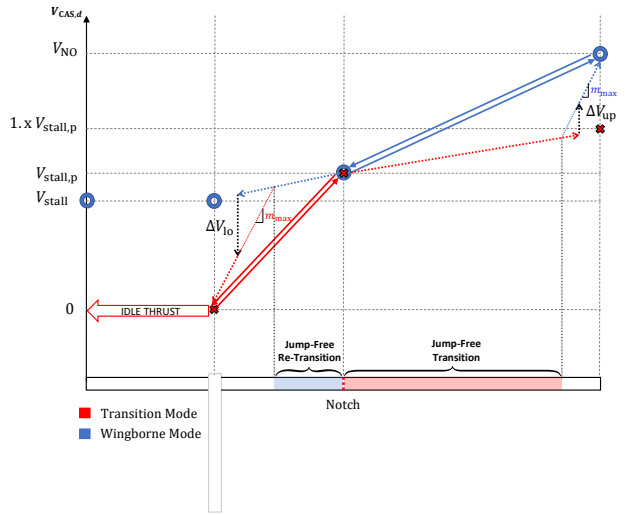

FIG 8. Overview of Left Control Inceptor Mapping for Transition Mode (red) and Wingborne Mode (blue)

the discrete mode switch and enables transition-free control authority transfer between different modes of operation while maintaining maximum authority and continuity of each mode. The continuity-based stick mapping is not discussed at this point but will be subject of a future publication.

Figure 8 shows an overview of the left control inceptor mapping for both the transition and the wingborne phase. The red crosses represent the target airspeed values for the transition phase, as is also shown in figure 7. The blue circles represent the target airspeed values during the wingborne phase. Note that below the notch the commanded airspeed during the wingborne mode drops to (but not lower than) the stall speed $V_{\mathrm{CAS},d} = V_{\mathrm{stall}}$ in order to initiate the re-transition.

The solid arrows on the right and left side of the notch level in figure 8 represent an exemplary stick path, where the transition and re-transition happen right behind and before the notch respectively, which represents the special case for which the left-sided and right-sided mapping gradients remain constant throughout the stick movement and the mapping reduces to a straight line in both directions.

The dotted line on the right side of the notch represents a stick path, where the switch into the wingborne mode happens outside the stick range, for which a jump-free transition can be achieved. The stick range for a jump-free transition is shaded in red in figure 8 and results from simple geometric construction by projecting the point onto the stick axis from which the maximum command of the wingborne mode V_{NO} would be reached in the transition mode with the maximum gradient m_{max}.

The dotted line on the left side of the notch represents a switch from the wingborne mode into the transition mode outside the stick range for a jump-free re-transition. Since pulling the stick below the notch is only a necessary but not sufficient condition for the re-transition [17], the switch from the wingborne mode into the transition mode can be initiated at any stick position below the notch. The gradient protecting increment ΔV_{lo} is added, such as to preserve the maximum allowed gradient m_{max} towards the new minimum airspeed limit $V_{\mathrm{min}} = 0$ in the transition phase. Analogously to the switch into the wingborne mode, the stick range enabling jump-free re-transition is shaded in blue and results from projecting the point onto the stick axis from which the minimum command of the transition mode $V_{\mathrm{min}} = 0$ would be reached in the wingborne mode with the maximum gradient m_{max}.

The proposed stick mapping provides intuitive control of the VTOL aircraft in the given flight modes by taking into account envelope protections and enables a smooth transition to and re-transition from the wingborne phase at any given situation.

The main disadvantage of the mapping is that a given stick position does not correspond to a fixed target velocity command, which might be desirable during the wingborne phase. An alternative strategy could combine the jump-free characteristics for the first half of the throttle area with a fixed stick to velocity mapping in the upper part of the stick area. This approach would considerably reduce the stick area for which a jump-free transition can be achieved, however, it would provide a constant stick mapping in the upper throttle stick area (which could potentially be marked-off by a second notch), such that the operator can command a fixed airspeed by placing the stick within the designated upper stick area.

2.3.2. Left Lateral Stick Channel During Wingborne Phase

During wingborne flight the lateral body-fixed specific force f_{By} is controlled, which is motivated by lateral aerodynamic forces encountered during sideslip conditions. As was already mentioned in subsection 2.2, the left lateral stick channel is mechanically locked above the detent notch. However, for the sake of completeness, a possible command mapping is introduced nonetheless. Deflections in this channel are interpreted as a desired lateral body-fixed load factor $n_{By,d}$ or aerodynamic sideslip angle $\beta_{\mathrm{aer},d}$ and are controlled by setting the target specific force to

$$f_{By,c} = n_{By,d} g = C_{fy,\beta} V_{\mathrm{CAS}}^2 \beta_{\mathrm{aer},d} \,, \tag{24}$$

with V_{CAS} denoting the calibrated airspeed and $C_{fy,\beta}$ summarizing the effects of mass, aerodynamic coefficients, and reference surface area for the lateral channel.

Note that in the case of a constant zero-command in this channel, aerodynamic turn coordination results at all times.

2.3.3. Right Longitudinal Stick Channel During Wingborne Phase

Pulling or pushing the right stick commands a climb or sink rate $\dot{h}_d$ respectively, just as for the transition and wingborne phase. The limits for the climb rate are governed by the available excess power of the transition aircraft at the given airspeed and altitude. It is of crucial importance to take into account the aircraft's propulsion power limit, since the command and control of excessive climb rates would lead to a rapid decrease of airspeed and hence to a possible stall condition or unanticipated re-transition and activation of the high-power lift system.
Both the airspeed and climb capability are ultimately governed by the available thrust and power characteristics of the system and hence cannot be controlled independently towards the border of the flight envelope. Figure 9 shows the qualitative relationship between airspeed and achievable maximum climb rate for propeller-driven aircraft. The underlying available propulsion power of the aircraft is assumed to be approximately constant over the airspeed.

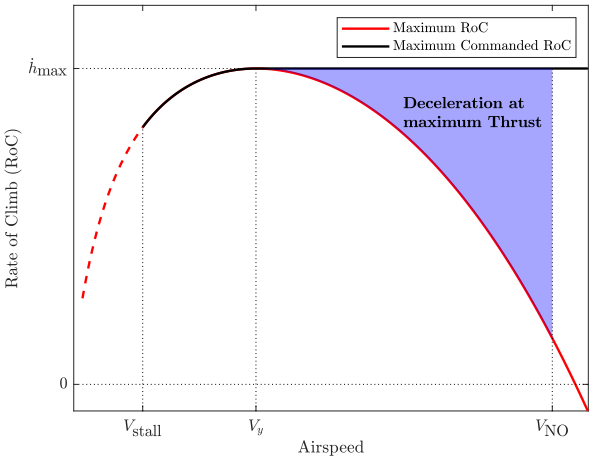

FIG 9. Rate of Climb for Different Airspeeds

For very low and high airspeeds climb performance deteriorates due to the dominating presence of induced and parasitic drag respectively. The overall maximum climb rate $\dot{h}_{\max}$ is achieved at an airspeed of V_y, at which maximum excess power is available.
For airspeeds lower than V_y pulling the right control inceptor commands climb rates up to the maximum achievable climb rate at the current airspeed, as is indicated by the black line in 9, which shows the commanded rate of climb for a maximum pull of the right stick. The target airspeed is held through auto thrust during the climb maneuver.
After exceeding the optimal climb speed V_y, the maximum climb rate that can be commanded by a complete pull of the right stick is fixed at $\dot{h}_{\max}$ and therefore exceeds the maximum vertical rate at which the aircraft can climb while keeping the airspeed constant.
Consequently, during a complete pull of the right control inceptor at an airspeed above V_y, the aircraft will initially start climbing while holding the airspeed constant up until the climb rate crosses the red curve in figure 9. At that point auto thrust will yield the maximum propulsion in order to track the target airspeed. The aircraft will then continue climbing with maximum thrust while decelerating until it reaches the optimal climb speed V_y and corresponding climb rate $\dot{h}_{\max}$. In this manner the transition aircraft always yields the absolute maximum climb rate $\dot{h}_{\max}$ when fully pulling the right stick at airspeeds greater or equal to V_y.
The demand in climb rate is actively protected by considering the deceleration margin towards the airspeed given by $V_{\text{prot}} = \min(V_{\text{CAS},d}, V_y)$ at maximum thrust condition. Given the total Energy of the system $E = \frac{1}{2}mV^2 + mgh$, the energy rate at full thrust yields

$$\dot{E} = mV\dot{V} + mg\dot{h} = (\cos(\alpha)T_{\max} - D)\,V\,, \tag{25}$$

with the aircraft's mass m, angle of attack α, maximum thrust force $T_{\max}$, and the drag D.
Considering (25), the commanded climb rate in wingborne flight is protected at any time by

$$\dot{h}_d \leq \frac{V}{g}\left(\underbrace{\frac{\cos(\alpha)T_{\max} - D}{m}}_{\substack{\text{Specific Excess Thrust} \\ \text{in Velocity Direction}}} - \dot{V}_{\text{prot}}\right), \tag{26}$$

where $\dot{V}_{\text{prot}} = K_V\,(V_{\text{prot}} - V)$ denotes the deceleration margin towards the protected airspeed in terms of a first order relationship with the time constant $\frac{1}{K_V}$.
Since the drag force in (26) cannot be measured directly, the specific excess thrust in the velocity direction can be estimated using inertial measurements and the remaining thrust capability of the system.
In order to command a sink rate, the right control inceptor is pushed forward. The maximum sink rate is only limited by avoiding over-speed conditions, which can occur if the system continues to gain speed while the thrust is already at an idle value.
During all flight phases from hover throughout the transition until the wingborne mode, the vertical channel is decoupled from the lateral channel through automatic attitude compensation during bank-to-turn maneuvers. Upon releasing the right stick, the current altitude is actively held by means of height hold functionality.

2.3.4. Right Lateral Stick Channel During Wingborne Phase

The response to lateral deflections of the right control inceptor is identical to the transition phase and yields a desired heading rate $\dot{\psi}_d$ (which corresponds to a desired turn rate due to coordination), which results from a coordinated turn with the target roll angle ϕ_c from (21). As was already mentioned in subsection 2.2, the limit of the achievable heading rate during a coordinated turn under the constraint of zero lateral body-relative acceleration $\dot{V}_{By} = 0$ was given in (23)

and depends on the required vertical acceleration capability $\ddot{h}_{\text{req}}$ and maximum available specific lift force $f_{\text{max}} = -f_{zB,\text{min}} > 0$ of the system.
During low speed operation, the available lift capability of the VTOL aircraft is approximately constant, as the required force is produced with the high-power lift system and is mostly independent of the current velocity. However, the maximum specific lift force capability during the wingborne phase is directly dependent on the current airspeed V and air density ρ and is given by

$$f_{\text{max}}(V) = \frac{1}{2m}\rho V^2 S C_{L,\text{max}}\,, \tag{27}$$

with the density ρ, airspeed V, the aircaft's mass m, reference wing area S, and its maximum lift coefficient $C_{L,\text{max}}$. Note that by definition the maximum lift force for $V = V_{\text{stall}}$ is equal to the aircraft's weight and therefore

$$f_{\text{max}}(V_{\text{stall}}) = g\,. \tag{28}$$

Hence, according to (23) the aircraft's lift capability upon entering the wingborne phase does not allow for any turn maneuver with $\ddot{h} \geq 0$. In order to still enable lateral controllability, the required vertical acceleration margin $\ddot{h}_{\text{req}}$ is therefore traded in for a minimum heading rate capability $\dot{\psi}_{\text{abs,min}}$. As a consequence, a full lateral deflection of the right control inceptor during horizontal flight at airspeeds close to the stall speed will initiate a turn maneuver that leads to a desired heading rate of $\dot{\psi}_d = \dot{\psi}_{\text{abs,min}}$ while yielding a (initial) sinking acceleration of

$$\ddot{h} = f_{\text{max}}\cos(\phi_c) - g\,, \tag{29}$$

with $\phi_c\left(\dot{\psi}_d\right)$ from (21).
This behavior prioritizes the lateral controllability over the vertical authority of holding the current altitude and hence allows for lateral flight path changes during low speed wingborne operation in order to avoid obstacles. As the aircraft's lift capability is increasing with growing airspeed V_{CAS}, lateral authority is adapted according to

$$\dot{\psi}_{\text{abs,max}} = \begin{cases} \dot{\psi}_{\text{abs,min}}, & \text{for } V_{\text{CAS}} < V_m \\ \dot{\psi}_{\text{abs,max,raw}}, & \text{for } V_{\text{CAS}} \geq V_m \end{cases}, \tag{30}$$

with the corner velocity

$$V_m = V_{\text{stall}}\sqrt{\frac{\ddot{h}_{\text{req}} + g}{g}} \tag{31}$$

and with the unprotected heading rate limit

$$\dot{\psi}_{\text{abs,max,raw}} = \frac{g}{g + \ddot{h}_{\text{req}}}\frac{1}{V_{Bx}}\sqrt{g^2\frac{V_{\text{CAS}}^4}{V_{\text{stall}}^4} - \left(\ddot{h}_{\text{req}} + g\right)^2}\,, \tag{32}$$

which follows from (23) with $f_{\text{max}} = g\frac{V_{\text{CAS}}^2}{V_{\text{stall}}^2}$.

Essentially, (30) sets the absolute command limit for the desired heading rate $\dot{\psi}_d$ to the minimum heading rate $\dot{\psi}_{\text{abs,min}}$ until the aircraft reaches enough airspeed such as to support the minimum heading rate $\dot{\psi}_{\text{abs,min}}$ while yielding the minimum vertical acceleration capability $\ddot{h}_{\text{req}} > 0$. From that airspeed on, the absolute maximum heading rate $\dot{\psi}_{\text{abs,max}}$ is governed by (32) and is approximately increasing linearly with growing airspeed.

3. VERIFICATION AND VALIDATION THROUGH SIMULATION OF EXECUTABLE SPECIFICATION MODEL

EASA has recently published the Proposed Means of Compliance with the Special Condition VTOL [18], in which they state that applicable validation activities for the flight control functions of VTOl aircraft include piloted real-time simulation.
Testing the proposed behavior and control concept directly in terms of use-case simulations represents a very effective way of validation, since it enables direct statements about the handling and general operation of the VTOL aircraft and does not rely on inferred statements based on existing requirements or metrics that might not be suitable or complete for VTOL operation.

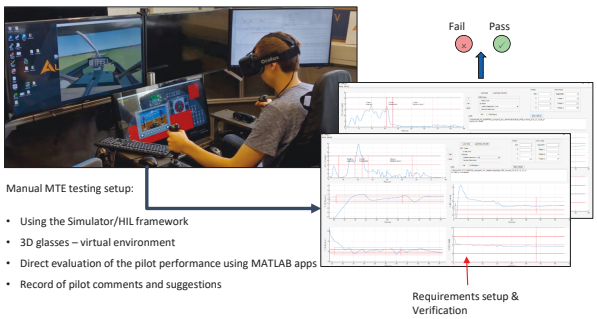

FIG 10. Pilot-in-the-Loop Simulation

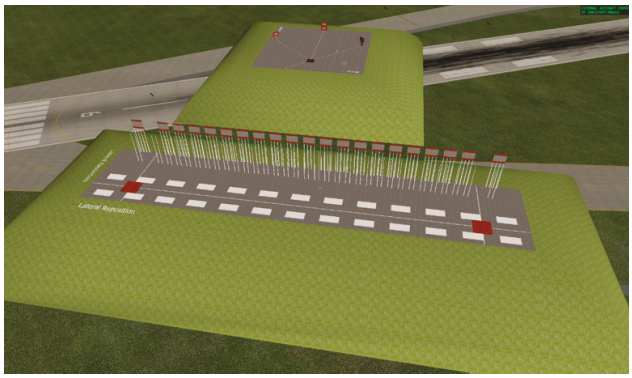

FIG 11. Mission Task Elements

Figure 10 shows the test setup with an executable *Design Reference Model* (DRM) incorporating the SVO concept from section 2 running in real-time on a desktop PC.

The DRM is a physically motivated specification of the closed-loop system behavior and reflects the vehicle response to pilot inputs in terms of a rigid-body simulation model which considers kinetic characteristics and constraints of the system, such as propulsion and lift characteristics, aerodynamic properties, mass, and Inertia. It is a system-architecture-agnostic representation of the final system and its behavior.
Hence, it does not rely on a detailed system and control architecture and can be used quite early in the design process in order to validate the aircraft's behavior and kinetic design with respect to the given application scenarios and proposed concept of operations.
Early validation is crucial when developing new systems due to the high amount of uncertainty regarding novel concepts and technologies. Being a disruptive technology, electric VTOL transition aircraft yield new operational scenarios, incorporate new behavioral aspects, and will hence require new methods and requirements for flying quality assessment.
The two control inceptors are read out via Matlab Simulink [19] and the corresponding behavioral response is visualized in a virtual environment. Additionally, the integration of a virtual-reality headset supports immersion and improves the perceived experience during testing.
Possible test scenarios include performing exemplary missions or conducting Mission Task Elements (MTEs), which are defined in [14]. Figure 11 shows the virtual set up of the mission tasks described in 3.11.1 and 3.11.8 in ADS-33E-PRF [14], where the former is used to "check [the] ability to transition from translating flight to a stabilized hover with precision and a reasonable amount of aggressiveness" [14, p. 27] and the latter one is used to "check roll axis and heave axis handling qualities during moderately aggressive maneuvering" [14, p. 34].
After completion of the mission tasks, pilots or operators use a Cooper-Harper rating scale to evaluate the handling qualities based on a set of criteria. Further discussion can also be found in [11].

4. CONCLUSION AND OUTLOOK

The proposed Simplified Vehicle Operations concept for onboard piloted VTOL transition aircraft yields intuitive handling and successful completion of virtual missions in the simulator, which has also been demonstrated in [11].
Rapid progress in automation technology such as sensors and embedded computer systems represents a key enabler for the successful development of highly augmented flight control functionality of VTOL aircraft. The high degree of automation and the substantial use of software changes the human role in the interaction with the vehicle from being a pilot to being a high-level operator to ultimately being a supervisor only, which changes the way one should assess and enforce emerging properties of the system such as handling qualities or safety [20].
Generating viable solutions for aircraft operation, design, and control constitutes a challenging task especially for VTOL transition aircraft. The wide operational envelope, high degree of functional automation, and insufficient experience with this type of vehicle makes it difficult to establish requirements as to how the system should behave and if the behavior is desirable and feasible both from an operational point of view and from a design or control point of view.
A systems-theoretic approach to the development of VTOL aircraft supports comprehensive consideration of their extensive functional aspects and yields a sound basis to cope with the inherent functional complexity of these systems.
Therefore, it is particularly important to approach the development of VTOL transition aircraft with systems-theoretic paradigms and to support it with the principles of model-based design. The successive analysis and simulation of models with increasing fidelity allows for stepwise validation of system aspects with increasing concretization (from behavioral and performance aspects to the architectural control design to the concrete implementation). This enables systematic creation, validation, and concretization of requirements in each phase throughout the system development and ensures the quality of the outcome.

References

[1] Alona Pukhova, Carlos Llorca, Ana Moreno, Qin Zhang, and Rolf Moeckel. Urban air mobility: another disruptive technology or just an insignificant addition. In *European Transport Conference. Dublin, Ireland*, 2019.

[2] Osborne Clarke. Battery technology advances are powering the rapid rise of electric vehicles. https://www.osborneclarke.com/insights/battery-technology-advances-powering-rapid-rise-electric-vehicles, March 26, 2021. Accessed on: July 03, 2021. [Online].

[3] NASA. Urban air mobility (uam) market study. https://ntrs.nasa.gov/api/citations/20190026762-/downloads/20190026762.pdf, November 2018. Accessed on: August 02, 2021. [Online].

[4] Uber. Redefining the future of safe on-demand air travel and transportation. https://uberpubpolicy.medium.com/fast-forwarding-to-a-future-of-on-demand-urban-air-transportation-f6ad36950ffa, October 27, 2016. Accessed on: June 05, 2021. [Online].

[5] Airbus. Rethinking urban air mobility. https://www.airbus.com/newsroom/stories/rethinking-urban-air-mobility.html, 2017. Accessed on: June 13, 2021. [Online].

[6] Aurora. Passenger air vehicle: Redefining the future of safe on-demand air travel and transportation. https://www.aurora.aero/pav-evtol-

passenger-air-vehicle. Accessed on: June 05, 2021. [Online].

[7] Volocopter. Urban air mobility: Innovation for a better city. https://www.volocopter.com/urban-air-mobility. Accessed on: July 03, 2021. [Online].

[8] Lilium. Architectural performance assessment of an electric vertical take-off and landing (e-vtol) aircraft based on a ducted vectored thrust concept. https://lilium.com/files/redaktion/refresh_feb2021-/investors/Lilium_7-Seater_Paper.pdf, April 07, 2021. Accessed on: June 05, 2021. [Online].

[9] Goodrich, Kenneth H. Simplified vehicle operations and airspace integration. http://www.nianet.org/ODM/September/32016.

[10] Thomas Lombaerts, John Kaneshige, and Michael Feary. Control concepts for simplified vehicle operations of a quadrotor evtol vehicle. In *AIAA AVIATION 2020 FORUM*, Reston, Virginia, 06152020. American Institute of Aeronautics and Astronautics. DOI: 10.2514/6.2020-3189.

[11] Daniel Dollinger, Philipp Reiss, Jorg Angelov, David Löbl, and Florian Holzapfel. Control inceptor design for onboard piloted transition vtol aircraft considering simplified vehicle operation. In *AIAA Scitech 2021 Forum*, 2021.

[12] Stefan A. Raab, Jiannan Zhang, Pranav Bhardwaj, and Florian Holzapfel. Proposal of a unified control strategy for vertical take-off and landing transition aircraft configurations. In *2018 Applied Aerodynamics Conference*, 2018.

[13] Guillermo Diaz Garcia, David Seiferth, Vitus Meidinger, Daniel Dollinger, Pranav Nagarajan, and Florian Holzapfel. Conduction of mission task elements within simulator flight tests for handling quality evaluation of an evtol aircraft. In *AIAA Scitech 2021 Forum*, page 1897, 2021.

[14] United States Army Aviation and Missile Command Aviation Engineering Directorate. Aeronautical design standard, performance specification, handling qualities requirements for military rotorcraft.

[15] Nicholas, O. P., and Bennett, P. J. Proposed wide envelope unified control concept for vectored thrust vstol aircraft. Technical Memorandum FS312, Royal Aircraft Establishment RAE, 1980.

[16] George Meyer and Luigi S. Cicolani. A formal structure for advanced automatic flight-control systems. 1975.

[17] Valentin A. Marvakov and Florian Holzapfel. Defining robust transition and re-transition procedures for unmanned fixed-wing vtol aircraft. In *AIAA Scitech 2021 Forum*, Reston, Virginia, 01112021. American Institute of Aeronautics and Astronautics. DOI: 10.2514/6.2021-1634.

[18] European Union Aviation Safety Agency. Special condition for small-category vtol aircraft. https://www.easa.europa.eu/sites/default/files/dfu/SC-VTOL-01%20proposed.pdf, 2020.

[19] MATLAB. *version 7.10.0 (R2010a)*. The MathWorks Inc, Natick, Massachusetts, 2010.

[20] Nancy G. Leveson. *Engineering a safer world: Systems thinking applied to safety*. The MIT Press, 2016.